

Electron Transfer from Cyt b_{559} and Tyrosine-D to the S_2 and S_3 states of the water oxidizing complex in Photosystem II at Cryogenic Temperatures

Yashar Feyziyev^{1,2}, Zsuzsanna Deák^{2,3}, Stenbjörn Styring² and Gábor Bernát^{2,4}

¹*Institute of Botany, 40 Patamdar Shosse, AZ-1073 Baku, Azerbaijan;*

²*Photochemistry and Molecular Science; Department for Chemistry – Ångström Laboratory, Uppsala University, Box 523, S-75120 Uppsala, Sweden;*

³*Institute of Plant Biology, Biological Research Center, H-6726 Szeged, Hungary;*

⁴*Plant Biochemistry, Ruhr-University Bochum, D-44780 Bochum*

Corresponding author: Stenbjörn Styring, Phone: +46-18-4716580; Fax: +46-18-4716844;

E-mail: Stenbjorn.Styring@fotomol.uu.se

Running Title: Electron transfer in Photosystem II

Keywords: EPR, photosystem II, water oxidation, S-states, tyrosine radical, cytochrome b_{559}

Abbreviations: Cyt, cytochrome; DAD, 3,6-diaminodurene; DMSO, dimethylsulfoxide;

EPR, electron paramagnetic resonance; HP and LP, high- and low potential, respectively;

MES, 2-(N-morpholino)ethanesulfonic acid; ML- S_2 , multiline EPR signal from the S_2 state of

WOC; P₆₈₀, the primary electron donor in PSII; PPBQ, phenyl-p-benzoquinone; PSII,

Photosystem II; WOC, water oxidizing complex; Y_D, the redox active tyrosine residue D2-

Y160; Y_D^{red} and Y_D[•] (= Y_D^{ox}), Y_D in the non-radical, reduced state and as neutral,

deprotonated radical, respectively; Y_Z, the redox active tyrosine residue D1-Y161, the major

electron donor to P_{680}^+ .

Abstract

The Mn_4CaO_5 cluster of photosystem II (PSII) catalyzes the oxidation of water to molecular oxygen through the light-driven redox S-cycle. The water oxidizing complex (WOC) forms a triad with Tyrosine_Z and P_{680} , which mediates electrons from water towards the acceptor side of PSII. Under certain conditions two other redox-active components, Tyrosine_D (Y_D) and Cytochrome b_{559} (Cyt b_{559}) can also interact with the S-states. In the present work we investigate the electron transfer from Cyt b_{559} and Y_D to the S_2 and S_3 states at 195 K. First, Y_D^\bullet and Cyt b_{559} were chemically reduced. The S_2 and S_3 states were then achieved by application of one or two laser flashes, respectively, on samples stabilized in the S_1 state. EPR signals of the WOC (the S_2 -state multiline signal, ML- S_2), Y_D^\bullet and oxidized Cyt b_{559} were simultaneously detected during a prolonged dark incubation at 195 K. During 163 days of incubation a large fraction of the S_2 population decayed to S_1 in the S_2 samples by following a single exponential decay. Differently, S_3 samples showed an initial increase in the ML- S_2 intensity (due to S_3 to S_2 conversion) and a subsequent slow decay due to S_2 to S_1 conversion. In both cases, only a minor oxidation of Y_D was observed. In contrast, the signal intensity of the oxidized Cyt b_{559} showed a two-fold increase in both the S_2 and S_3 samples. The electron donation from Cyt b_{559} was much more efficient to the S_2 state than to the S_3 state.

Introduction

Photosystem II (PSII), the light-driven water-plastoquinone oxidoreductase (Fig. 1, [1]), is a key enzyme of photosynthesis and energy transduction in particular – and life on Earth in general. The most recent, highly resolved (1.9Å) three-dimensional structure of PSII [2] provides a very detailed picture of the organization of the supercomplex including precise localization of cofactors, amino acid side chains, water molecules and also the structure of the Mn_4CaO_5 water-oxidation catalytic center (WOC). According to the current view, WOC forms a triad with the primary donor of PSII, P_{680} and a redox-active tyrosine residue, Y_Z (D1-Y161). Electron transfer in PSII starts with the excitation of P_{680} and subsequent charge separation followed by several secondary electron transfer steps (for a review, see [3]). These involve the sequential reduction of pheophytin (Phe) and plastoquinone electron acceptors (Q_A , Q_B), on the PSII acceptor side and sequential oxidation of Y_Z and WOC on the donor side (Fig. 1). The catalytic site of WOC is a Mn_4CaO_5 cluster which accumulates four positive charges (after four charge separations) during the cycle of water oxidation, the so-called S-cycle [3-6]. This S-cycle involves five intermediate redox states (from S_0 to S_4) where S_0 is the most reduced state and S_4 state is a transient intermediate between S_3 and S_0 [7]. While the S_0 and S_1 states are quasi-stable and stable, respectively, the S_2 and S_3 states are energetically unstable and decay to S_1 state in the dark. The accumulation of oxidizing equivalents on the WOC is accompanied by proton release/relocation [5, 8-13, and references therein] in which process apparently the Y_Z – D1-H190 interaction plays a key role. The spatial arrangement of the Mn_4CaO_5 cluster suggests that Mn_4 , the manganese located outside the cubane in connection with Y_Z *via* a hydrogen-bond network [2], may provide the catalytic site for water oxidation.

Besides the components of the major electron transport route (i.e. from water to plastoquinone), PSII also have several components involved in auxiliary electron transport

routes, which are believed to play important roles in photoprotection and photoactivation [14-19, see also 20, 21; for a recent review see 22]. In these reactions, at least under certain circumstances, the second redox active tyrosine Y_D (D2-Y160) and cytochrome *b*₅₅₉ (Cyt *b*₅₅₉) participate in electron transfer to the WOC [14, 23-27]. Electron transfer from Y_D to the S₂ and S₃ states of WOC has been well studied at room temperature [23, 27]; some data on S-state dependent oxidation of Cyt *b*₅₅₉ is also available [28]. According to our previous results, these types of electron transfer also occur at 275 K and 245 K [29]. The earlier studies have revealed that at room temperature and at 275 K both the S₂ and S₃ states dominantly decay *via* electron donation from (pre-reduced) Y_D when charge recombination with acceptor side components is prevented [23, 29]. Involvement of Cyt *b*₅₅₉ in the electron transfer process comes into play at those temperatures only when other routes are inactivated or not fully functional [14, 17, 30]. Y_D is almost fully oxidized during the decay of the higher S-states at \geq 275 K. Differently from this the Y_D oxidation is only fractional (up to 70%) at 245 K and in about 20% of the PSII centers Cyt *b*₅₅₉ exclusively reduces the S₂ state [29].

Our present work extends these studies to 195 K and provides unexpected information regarding the electron transfer reactions between Y_D, Cyt *b*₅₅₉ and the WOC in the S₂ and S₃ states.

Materials and methods

Preparations of PSII membranes. PSII enriched membrane fragments (BBY-type) were prepared from hydroponically grown greenhouse spinach [31] with modifications according to [32]. The isolated membranes were resuspended in 50 mM MES-NaOH buffer (pH 6.2) supplemented with 35 mM NaCl and 300 mM sucrose (medium A) at a chlorophyll concentration of 4 mg/ml and stored at liquid nitrogen until use. In the presence of 200 μ M PPBQ the oxygen evolution rate of this type of preparation was about 450 μ mol of O₂ (mg

$\text{Chl})^{-1}\text{h}^{-1}$.

Preparation of EPR samples. Tyrosine $\text{Y}_\text{D}^\bullet$ and Cyt b_{559} were reduced chemically by sodium ascorbate and 3,6-diaminodurene (DAD) treatment [29]. First, PSII membranes were resuspended in medium A at a chlorophyll concentration of 1 mg/ml and kept in darkness at room temperature for 30 min. Then, 5 mM Na-ascorbate and 1 mM DAD were added and the suspension was incubated for another 30 min. After these incubations the suspension was diluted 8 to 10-fold with buffer A and precipitated by a centrifugation at 30,000g ($t = 20$ min) – this washing procedure was repeated twice. Finally, the pellet was resuspended in buffer A at a chlorophyll concentration of 4 mg/ml. The chemically reduced PSII membranes ($\text{Y}_\text{D}^{\text{red}}$ PSII) were transferred into calibrated EPR tubes and 0.5 mM PPBQ (dissolved in DMSO; final DMSO concentration in the probes is 2% (v/v)) was added. It is critical that all of these steps are performed in complete darkness to prevent photochemical reoxidation of Y_D and Cyt b_{559} . One and two (5 Hz) short (7 ns) saturating light flash(es) of a Nd:YAG laser (400 mJ/pulse, 532nm) was/were then applied at 20°C to induce the $\text{Y}_\text{D}^{\text{red}}\text{S}_1 \rightarrow \text{Y}_\text{D}^{\text{red}}\text{S}_2$ and $\text{Y}_\text{D}^{\text{red}}\text{S}_1 \rightarrow \text{Y}_\text{D}^{\text{red}}\text{S}_3$ transitions, respectively. After the flashes, the samples were frozen quickly (within 1 s) in an ethanol/dry ice mixture, and then rapidly transferred into liquid nitrogen where they were stored until use. Dark (non-flashed) samples (in the $\text{Y}_\text{D}^{\text{red}}\text{S}_1$ state) were also prepared as controls.

EPR samples with oxidized Y_D ($\text{Y}_\text{D}^\bullet$) were also prepared. In this case, complete $\text{Y}_\text{D} \rightarrow \text{Y}_\text{D}^\bullet$ oxidation was achieved by short (~1 min) exposure to room light followed by 5 min dark incubation at 20°C, which allows the decay of higher S-states, prior to the addition of PPBQ. The maximal signal amplitude of the $\text{Y}_\text{D}^\bullet$ radical was identical in the non-treated samples and in the ascorbate/DAD-treated samples after Y_D had been reoxidised by extensive illumination. The maximal amplitude of the S_2 state multiline EPR signal (ML- S_2) was achieved by continuous illumination (8 min white light, using an 800 W projector lamp) of the samples in

an ethanol-dry ice bath (T=195 K).

EPR spectroscopy. EPR measurements were performed using a Bruker ESR-500 spectrometer, equipped with an ST4102 standard cavity, an Oxford-900 cryostat and an ITC-503 temperature controller. ML-S₂ was recorded at 7 K with an instrumental setting of 13.1 mW microwave power and 20 G field modulation amplitude. Its amplitude was estimated as a sum of the amplitudes of three hyperfine peaks between 2900 G and 3100 G (see Fig. 2B). The EPR signals of Y_D[•] and oxidized Cyt b₅₅₉ were recorded at 15 K. The Y_D[•] radical was detected at a microwave power of 1 μW combined with a field modulation amplitude of 3.2 G, while 5.3 mW microwave power and 16 G field modulation amplitude was used for the detection of oxidized Cyt b₅₅₉. The amplitude of the low field peak (see Fig. 2A) was used to estimate the amplitude of Y_D[•], while oxidized Cyt b₅₅₉ was quantified by integrating of its g_z (g ≈ 3) peak (see Fig. 3). The amplitude of the recorded EPR signals was fitted using kinetic models published in [29].

Results

EPR spectra of chemically reduced PSII. When the alternative electron donor Y_D is reduced (Y_D^{red}), the flash-induced period-4 turnover of the S-cycle is rapidly desynchronized due to competing electron transfer from Y_D^{red} resulting in high probability of misses. The effect is very pronounced in samples which are only partially synchronized in the the S₁ state, e.g. by relatively short dark-incubation without applying any preflash, and, therefore with high (up to ~25%) S₀ contamination [4, 23]. However, it has been shown [23, 24] that prolonged dark-incubation results in an S₀Y_D[•] → S₁Y_D^{red} conversion. This protocol was also applied before the DAD/ascorbate-treatment in the current work, stabilizing the majority of the PSII complexes in the S₁ state. Therefore, after one and two powerful laser flashes followed by rapid freezing these samples are dominantly in the S₂Y_D^{red} and S₃Y_D^{red} states (see

below).

Some EPR spectra of DAD/ascorbate-reduced samples are shown in Figs. 2 and 3. The absence of any residual radical signal from Y_D^\bullet in the 0-flash sample (Fig. 2A, spectrum *a*) shows that the applied protocol results in a fully reduced Y_D population. Application of one and two laser flashes on such samples induced the appearance of a small tyrosine Y_D^\bullet radical signal (spectra *b* and *c*) with a size of 10-14% and 15-16% of the maximal signal intensity, which shows that the majority of the PSII centers were in $Y_D^{\text{red}}S_2$ and $Y_D^{\text{red}}S_3$, respectively, in these samples. Complete oxidation of tyrosine Y_D was easily achieved by the usual 1 min light – 5 min dark treatment (see Materials and methods) of the 0-flash sample (Fig. 2A, spectrum “*max*”). The spectrum was very similar to those of oxidized Y_D recorded in samples not treated with DAD and ascorbate (data not shown).

Fig. 2B shows the ML- S_2 spectra recorded in the same samples as in Fig. 2A. In the 0-flash sample (spectrum *a*) there was no detectable contribution of ML- S_2 which demonstrates that the majority of the PSII centers were indeed stabilized in the S_1 state by prolonged dark incubation. Illumination of this sample at 200 K induces a typical ML- S_2 (not shown). The amplitude of this signal was used as a control for determining the S_2 and S_3 population size in the samples illuminated by one and two flashes (spectra *b* and *c*), respectively. Different from the 0-flash sample, the EPR spectrum of the sample frozen after one laser flash shows an ML- S_2 (spectrum *b*). The amplitude of the recorded signal was increased only about 15-20% by a subsequent illumination at 200 K (data not shown), which shows that the sample was dominantly (80-85%) in the S_2 state, with about 15-20% in the S_1 state. The two-flash sample also shows an ML- S_2 signal with a size of 40-50% of the maximal signal intensity (Fig. 2B, spectrum *c*). Subsequent illumination of this sample by continuous white light at 200 K did not induce increase the ML- S_2 intensity (data not shown) indicating that very few if any

centers remained in S_1 state after two laser flashes. This observation also implies that 50-60% of the PSII complexes were in the S_3 state after the two flashes. The existence of a large fraction of S_2 centers in the two-flash sample can be partially explained by ordinary misses and partially by oxidation of Y_D^{red} (15-16%, see above) which delivers a remarkable fraction of the centers back to the S_2 -state before the sample is frozen. As a summary, we found that about 80-85% and 50-60 % of the PSII centers were in the $Y_D^{\text{red}}S_2$ and $Y_D^{\text{red}}S_3$ states after one and two flash(es), respectively.

Different from the Y_D^{\bullet} radical and ML- S_2 , which were completely absent in the 0-flash sample, an EPR signal of oxidized Cyt b_{559} was detected in this sample (not shown). This signal belongs to the so-called low-potential (LP) form of Cyt b_{559} (with a characteristic g_z peak at $g = 2.97 / 2255$ G) which can be observed in all types of (even inactivated) PSII preparations (see e.g. [17, 30, 33-37]). Applying either one or two powerful laser flashes did not induce any change in the shape or intensity of this signal (Figs. 3A and B, spectra *a*) which indicates that no significant (further) oxidation of Cyt b_{559} occurred during the preparation of the 1- and 2-flash samples.

Decay of the $Y_D^{\text{red}}S_2$ state at 195 K. The 0-flash (100% $Y_D^{\text{red}}S_1$), 1-flash (80-85% $Y_D^{\text{red}}S_2$) and 2-flash (50-60% $Y_D^{\text{red}}S_3$) samples were incubated at 195 K for up to 6-8 months in complete darkness and EPR spectra with the settings of the ML- S_2 , Y_D^{\bullet} and Cyt b_{559} were recorded regularly at various time points during this prolonged dark incubation at cryogenic temperature.

In the 1-flash sample which was initially dominated (80-85%) by the $Y_D^{\text{red}}S_2$ state, the time-course of the amplitude of ML- S_2 followed a single exponential decay and after 163 days of dark incubation at 195 K only about 40% of the original signal intensity remained (Fig. 4A, closed circles). Most likely, the disappearance of the ML- S_2 indicates the

corresponding formation of the S_1 state. Simultaneous detection of the Cyt b_{559} and Y_D^\bullet signals shows that the decay of ML- S_2 is accompanied with the oxidation of Cyt b_{559} (Fig. 3A, spectra b and c ; Fig 4A, closed triangles) and Y_D (Fig 4A, closed squares). Noticeably, oxidation of Cyt b_{559} during the dark incubation of the sample at 195 K is manifested as a formation and subsequent gradual increase of a signal component of Cyt b_{559} peaking at $g = 3.05/2205$ G. This component belongs to the (oxidized) high-potential (HP) form of Cyt b_{559} . In contrast, the intensity of the LP signal remained constant. As a result, the Cyt b_{559} LP form is observed as a shoulder at the high-field side of the composite signal after >40 days of dark incubation (Fig. 3A, spectra b and c). While the signal intensity of the oxidized Cyt b_{559} increased from 50% up to 85% of its maximal intensity, the Y_D^\bullet signal increased only slightly (from 16% to 20% of its maximal intensity) after 163 days of dark incubation at 195 K.

The rise kinetics of the Cyt b_{559} signal ($k = 0.0168 \text{ d}^{-1}$) was similar to that of the S_2 decay ($k = 0.0236 \text{ d}^{-1}$) while the rise kinetics of Y_D^\bullet ($k = 0.0051 \text{ d}^{-1}$) was much slower. In addition, the sum of the rate constants for the Cyt b_{559} and Y_D oxidation is very close to the rate constant of the S_2 decay which indicates that participation of other electron donor(s) in this decay process is very unlikely. All of these data show that the majority (>70%) of the S_2 centers were reduced by Cyt b_{559} at 195 K in the 1-flash sample and the $Y_D^{\text{red}}S_2 \rightarrow Y_D^\bullet S_1$ conversion has only a minor role in this process. This conclusion is also supported by a plot of the intensity of Cyt b_{559} signal vs. the ML- S_2 intensity (Fig. 4B). The data points here show an almost linear relationship between the two signals which indicates that Cyt b_{559} is the major electron donor to S_2 at 195 K. However, the slope of the curve is > -1 and a better fit can be achieved by a broken line. Both these effects show the minor involvement of another donor. Our measurements indicate that this is most likely Y_D .

Decay of the $Y_D^{\text{red}}S_3$ state at 195 K. The kinetic behavior of the 2-flash sample which was

dominated by $S_3 Y_D^{\text{red}}$ (Fig. 5A) is quite different from that of the 1-flash sample. During the first 15-20 days of incubation, the ML- S_2 signal showed a slight increase (Fig. 5A, inset) which was followed by a slow decay during the subsequent incubation period. This indicates simultaneous formation and elimination of the S_2 state, i.e., during the $S_3 \rightarrow S_2$ and $S_2 \rightarrow S_1$ decays, respectively, and also that the $S_3 \rightarrow S_2$ decay is faster than the $S_2 \rightarrow S_1$ decay. This conclusion is also supported by fitting of the multiline signal intensities by a kinetic model used in our earlier work [29]. Such fitting (Fig. 5A, inset) results in a high rate constant for the $S_3 \rightarrow S_2$ decay ($k_1 = 0.055 \text{ d}^{-1}$) while the rate constant for the $S_2 \rightarrow S_1$ decay is approximately ten-fold lower ($k_2 = 0.0054 \text{ d}^{-1}$). The inset in Fig. 5B shows the relatively fast decay of the S_3 state as calculated from the initial S_3 population (50-60%, see above) and k_1 .

The rise of oxidized Cyt b_{559} (Fig. 3B, spectra *b* and *c*, Fig. 5A, closed triangles) followed a similar monoexponential kinetics in the 2-flash sample as in the 1-flash sample, rising from 50% up to 90% of its maximal intensity, with a rate constant of $k = 0.0083 \text{ d}^{-1}$. This is in the same range as for the $S_2 \rightarrow S_1$ decay in this 2-flash sample (see above). Here again, formation of the Cyt b_{559} HP signal was observed while there were no changes in the Cyt b_{559} LP signal intensity (Fig. 3B). Similar to in the 1-flash sample, the intensity of the Y_D^\bullet radical signal in the 2-flash sample showed only a slight increase during the prolonged dark incubation at 195 K (from 15-16% to 25-26%). This rise apparently consists of two kinetically distinct phases.

By comparison of the EPR signal intensities in the 1- and 2-flash samples it seems that reduced Cyt b_{559} and Y_D can donate electrons both to the S_2 and S_3 state at this temperature, but this electron donation is much more efficient to the S_2 state. Again, similar to in the 1-flash sample, the major electron donor is Cyt b_{559} while Y_D has only a minor role in this decay process at this temperature.

These conclusions are well supported by the plot showing the intensity of the Cyt b_{559} signal vs. the predicted S_3 population size (Fig. 5B). This plot (Fig. 5B) shows a hyperbolic

relationship between the Cyt b_{559} signal and the S_3 population: Almost no change in the Cyt b_{559} signal intensity was observed during the initial (< 30 d) part of the S_3 decay, while the S_3 population decreased from 55% to ~15% of the centers. This period is then followed by a very large Cyt b_{559} oxidation during the subsequent incubation. In this period the S_3 state decayed only from 15% to 0%. This complex oxidation of HP Cyt b_{559} is very different from the analogous plot for the S_2 decay (Fig. 4B) which shows an almost linear correlation between the intensities of Cyt b_{559} and ML- S_2 signal.

Independently of the initial S-state (i.e. S_2 or S_3), after two laser flashes and subsequent freezing, earlier or later, all of the centers are at same stage in the S_2 state during the long-term incubation at 195 K and decay thereafter ultimately to the S_1 state. Thus, by combining Figs. 5A and B (i.e. the measured and predicted S_2 and S_3 populations, respectively) the population of the centers which have already left the S_2 state (i.e. the S_1 population) can be also estimated. A plot showing the intensity of the Cyt b_{559} signal vs. the estimated S_1 population size is shown in Fig. 5C. Not surprisingly, the intensity of the Cyt b_{559} signal increases with the number of completed $S_2 \rightarrow S_1$ transitions. However, the formation of oxidized Cyt b_{559} is biphasic: the intensity of the Cyt b_{559} signal increases only in a small extent until ~50% of the centers decays to S_1 . Then, a relatively small (~20%) increase of the S_1 population is accompanied by a remarkable (30%) increase of intensity of the Cyt b_{559} signal. The biphasic character of the plot, like in the 1-flash samples (Fig. 4B), indicates again the minor involvement of another donor in the $S_2 \rightarrow S_1$ decay – most likely Y_D .

Astonishingly, the plot in Fig. 5C is very similar to that in Fig. 4B in two major aspects. First, both plots have a biphasic character (see above) with a turning point at 50-55% S_1 population. Formation of the S_1 state below and above this population size is accompanied with a moderate and prominent oxidation of Cyt b_{559} , respectively. Second, the 65% and 77% increase in the S_1 population (=decay of/through the S_2 state) during the decays of the higher

S-states in the 1-flash and 2-flash samples is accompanied by 36% and 41% increase, respectively, of the intensity of Cyt b_{559} EPR signal. This shows a fairly linear correlation between the number of centers which have performed an ($S_3 \rightarrow$) $S_2 \rightarrow S_1$ decay and extent of Cyt b_{559} oxidation. A very clear conclusion from these observations is that HP Cyt b_{559} is a much more potent electron donor to the S_2 state than to the S_3 state at 195 K (see below).

Discussion

The interesting electron transfer reactions between the WOC in various S-states and the auxiliary electron donors Y_D and Cyt b_{559} have now been followed at several incubation temperatures. It was early found that Y_D^{red} could donate an electron to either of the S_2 (after 1 flash) or S_3 states (after 2 flashes) with very similar kinetics at room temperature. In those studies, oxidation of HP Cyt b_{559} was never observed [23, 24, 38, 39] and it was concluded that the electron transfer involved a series of charge equilibria between Y_D , P_{680} , Y_Z and the WOC [24, 29; see also 25].

The same reactions were later studied at 275 K and 245 K which revealed that Y_D^{red} and HP Cyt b_{559} actually both could function as electron donors to the higher S-states. However, the competition was highly temperature dependent. In this study [29] we could prove that both Y_D^{red} and HP Cyt b_{559} became oxidized to significant extent during dark incubation at 245 K of samples initially enriched in the S_2 or the S_3 state. It was also found that HP Cyt b_{559} probably could work as a direct donor to the S_2 state at this temperature. This was interpreted as that Cyt b_{559} competes with Y_D in electron donation to the higher S-states (i.e. S_2 and S_3) directly or *via* a redox equilibrium with other PSII cofactors (e.g. components of the Car/Chl $_Z$ - P_{680} - Y_Z pathway).

The present work extends this earlier work and addresses these charge transfer reactions between the auxiliary electron donors and the water oxidizing complex of PSII in different S-

states at 195 K.

To be able to follow the interaction between Y_D and the higher S-states we initially reduced Y_D and HP Cyt b_{559} chemically. Then PSII was advanced to either the S_2 or the S_3 state by exciting samples with one or two short laser flashes. Although the decay of the S_2 and S_3 states is much slower at 195 K than at 245 K or 275 K, our present data obtained by monitoring the amplitude changes of ML- S_2 show that the kinetic pattern of the S_2 and S_3 decays are essentially the same at all of these temperatures.

In the 1-flash sample (enriched in the $Y_D^{\text{red}}S_2$ state) the decay of the ML- S_2 follows a monoexponential kinetics. At 195 K this reaction occurs in the time-scale of months. The decay displays electron transfer from a neighboring PSII component(s) to S_2 resulting in the S_1 state and an oxidized donor. (We discuss the nature of this donor below). Importantly, due to the presence of the artificial electron acceptor PPBQ, charge recombination (with acceptor side components) as a reason of the decay of higher S-states can be excluded.

In the 2-flash sample (dominated by the $Y_D^{\text{red}}S_3$ state) changes of the ML- S_2 follow a complex kinetic behavior during the S_3 state decay with a rising and a decaying phase, similar to the case observed at higher temperatures (≥ 245 K) [23, 29, 40], although the rising phase of ML- S_2 is less pronounced at 195 K. This complex behavior can be explained by parallel formation and elimination of the S_2 state during the $S_3 \rightarrow S_2 \rightarrow S_1$ decay pathway, in which, despite one more positive charge being generated, the expected end product is also the S_1 state (see scheme in refs 23 and 29). Similar to in the 1-flash sample, the ML- S_2 decays very slowly (i.e. in the time scale of months) during the dark incubation and a large fraction of PSII centers are still in S_2 state after 8 months of storage.

Although the kinetic pattern of the S_2 and S_3 decays are similar at 195 K, 245 K, 275 K and room temperature, the electron donor(s) that participate in these reactions are different at the different temperatures. At 275 K the S_2 state is exclusively reduced by Y_D . This also holds

for the S_3 state when reduced Y_D is present. Interestingly an unidentified, EPR-silent PSII component reduced the S_2 state in the sequence $Y_D^{\text{red}}S_3 \rightarrow Y_D^{\bullet}S_2 \rightarrow Y_D^{\bullet}S_1$ – without any measurable contribution of Cyt b_{559} in both cases. This was in agreement with literature data [24, 38] where quantitative oxidation of Y_D^{red} was observed concomitantly with the decay either of the S_2 and S_3 states and, thus, Y_D^{red} was suggested as an efficient electron donor to both of the S_2 and S_3 states.

Differently from this, our previous investigations at 245 K revealed that Cyt b_{559} also participates in the reduction of the S_2 and S_3 states. At this temperature still, Y_D^{red} was the major EPR-active electron donor and only about 20% of the centers were reduced by Cyt b_{559} . Despite this, our data indicated that Cyt b_{559} was an equally efficient donor to the S_2 state as Y_D^{red} . In contrast, when Y_D^{red} was present, it totally outcompeted Cyt b_{559} during reduction of the S_3 state.

The present results clearly demonstrate that at 195 K the major electron donor to the S_2 state is Cyt b_{559} while the electron donation from Y_D^{red} plays only a minor role both to the S_2 and the S_3 state. This was manifested by the very small increase of the intensity of the Y_D^{\bullet} radical signal. These observations are in good agreement with the relatively high activation energy of the $Y_D^{\text{red}}S_2 \rightarrow Y_D^{\bullet}S_1$ and $Y_D^{\text{red}}S_3 \rightarrow Y_D^{\bullet}S_2$ reactions (0.57 and 0.67 eV, respectively). As a consequence, Y_D cannot compete efficiently in donating electrons to the S_2 and S_3 states. Instead Cyt b_{559} becomes the dominant electron donor at 195 K. This holds at least for the S_2 state where oxidation of HP Cyt b_{559} correlates well with the decay of the S_2 state both in 1- and 2-flash samples.

It is interesting why Cyt b_{559} is an efficient donor to the S_2 state but not to the S_3 state at 195 K. There are several plausible explanations – all of them are related either to the different nature of the S_2 and S_3 states or of the $S_1 \rightarrow S_2$ and $S_2 \rightarrow S_3$ transitions (and *vice versa*: the reverse $S_2 \rightarrow S_1$ and $S_3 \rightarrow S_2$ decays). Independent from the exact reason, the S_3 state is

reduced by another – unknown – donor relatively quickly at 195 K and the resulting S₂ center then decays back to S₁ as in the 1-flash samples.

The S₂ and S₃ states differ not only in numbers of accumulated positive charges (holes) but also in charge distribution, midpoint redox potential and probably also in Mn-coordination. Regarding charge distribution, there has been a long standing discussion in the literature on the oxidation state of the Mn₄CaO₅ catalytic center. The important question is whether all of the positive charges in the S₃ state are localized on manganese ions or if one of these charges is localized on a neighboring ligand (for reviews, see [41-44]). A multistate equilibrium between metal- and ligand-centered oxidation in the S₂ → S₃ transition has also been proposed [43, 45, 46]. Neither the (sole) oxidation of a manganese atom nor of a ligand seemingly can explain the observed S-state dependent difference in the Cyt *b*₅₅₉ → WOC electron donation to the S₂ or S₃ state. This, because the positive charge which is present in the S₂ state, is also present in the S₃ state. In contrast, the proposed multistate equilibrium model may offer an explanation. This model suggests a coexistence of three different states: M₃L₀W₀ ⇌ M₂(LW)₀ ⇌ M₁L₀W₂, where the subscripts of M, L and W represent the oxidation level of the metal (manganese) center, ligand, and substrate, respectively. Noteworthy, in the M₁L₀W₂ state the manganese cluster is reduced by one electron more than in the S₂ state, therefore, in the (theoretical) case when this is the dominant form of the S₃ state, its reduction *via* Cyt *b*₅₅₉ might be impossible at 195 K when transition/proton tautomerism to other forms might be prevented.

Very similar conclusion (i.e. prevented electron donation from Cyt *b*₅₅₉ to the S₃ state) could also be drawn from the reported large structural rearrangement during the S₂ → S₃ transition which was interpreted as a formation of a new μ-oxo bridge between two manganese ions of the Mn₄CaO₅ catalytic center [47] as at 195 K the reverse structural change might be inhibited.

The S_2 and S_3 differ in many aspects both with respect to electronic, protonic and structural properties. The midpoint redox potential of both couples is about 900-950 mV [24, 48] and the S_3 state is thought to be slightly less oxidizing than the S_2 state at neutral pH [49]. Although this small difference in the redox potentials may involve alterations in the S_2 and S_3 redox kinetics at low temperatures we find the difference too small to explain why Cyt b_{559} is able to reduce the S_2 state but unable to reduce the S_3 state at 195 K.

A different, but maybe more likely explanation involves the protonation state in the WOC. The $S_1 \rightarrow S_2$ transition involves only a one step oxidation of Mn in the WOC while no proton movement occurs (see e.g. [7, 10, 11, 13]). Therefore the S_1 transition occurs smoothly at cryogenic temperatures [40], e.g. illumination at 200 K is a standard protocol to drive the $S_1 \rightarrow S_2$ transition (see e.g. Results). This will also hold for the backwards reaction and, since Cyt b_{559} can provide an electron, the electron transfer from Cyt b_{559} to WOC in the S_2 state will function well.

In contrast, the $S_2 \rightarrow S_3$ transition involves both oxidation of and proton release from the WOC. Therefore the $S_2 \rightarrow S_3$ transition is more sensitive to temperature. This difference will also steer the backwards reaction. Naturally, the released proton must come back during the $S_3 \rightarrow S_2$ decay. This holds irrespective of which electron donor is available. This proton transfer (release or uptake) is likely coupled to electron transfer. Therefore, the impairment proton transfer, for example at lower temperatures should impair also the electron transfer. If this was the case, Cyt b_{559} will not be able to donate an electron to the S_3 state under this condition.

The *bona fide* redox equilibria between the major and auxiliary donor side components occur *via* Y_Z and P_{680} [15, 25, 29], and it is generally believed that the $Y_Z \rightarrow$ WOC electron transport is coupled to proton movement between Y_Z and D1-His190 in both S_2 and S_3 (for a review, see [50]). The results in our recent and previous work [29] clearly show that the S_2

state, which is clearly reduced primarily by equilibrium with Y_Z at ≥ 275 K, can still be reduced by Cyt b_{559} at ≤ 245 K. This strongly suggests the existence of a direct electron transfer pathway from Cyt b_{559} to the WOC at cryogenic temperatures (≤ 245 K) in which Cyt b_{559} can reduce the S_2 state without the involvement of a redox equilibrium between P_{680} , Y_Z and WOC. Our findings are summarized in Fig. 6.

Acknowledgements

This work was supported by grants from the Swedish Energy Agency, the Swedish Research Council, the EU/Energy Network project SOLAR-H2 (FP7 contract no. 212508), and the EC Program “Improving Research Potential and Socio-Economic Knowledge Base” (MCFI-2000-01465).

References

- [1] T.J. Wydrzynski, K. Satoh (Eds.), Photosystem II: The light-driven water:plastoquinone oxidoreductase, Springer, Dordrecht, the Netherlands, 2005.
- [2] Y. Umena, K. Kawamaki, J.R. Shen, N. Kamiya, Crystal structure of oxygen evolving photosystem II at an atomic resolution of 1.9 Å, *Nature* 473 (2011) 55-60.
- [3] G. Renger, T. Renger, Photosystem II: The machinery of photosynthetic water splitting, *Photosynth. Res.* 98 (2008) 53-80.
- [4] B. Kok, B. Forbush, M. McGloin, Cooperation of charges on photosynthetic O_2 evolution, *Photochem. Photobiol.* 11 (1970) 457-476.
- [5] H. Dau, C. Limberg, T. Reier, M. Risch, S. Roggan, P. Strasser, The mechanism of water oxidation: From electrolysis via homogenous to biological catalysis, *ChemCatChem* 2 (2010)

724-761.

[6] F. Muh, A. Zouni, Light-induced water oxidation in photosystem II, *Front. Biosci.* 16 (2011) 3072-3132.

[7] M. Haumann, P. Liebisch, C. Müller, M. Barra, M. Grabolle, H. Dau, Photosynthetic O₂ formation tracked by time-resolved X-ray experiments, *Science* 310 (2005) 1019-1021.

[8] E. Schlodder, H.T Witt, Stoichiometry of proton release from the catalytic center in photosynthetic water oxidation – Reexamination by a glass electrode study at pH 5.5-7.2, *J. Biol. Chem.* 274 (1999) 30387-30392.

[9] C.W. Hoganson, N. Lydakis-Simantiris, X.S. Tang, C. Tommos, K. Warncke, G.T. Babcock, B.A. Diner, J. McCracken, S. Styring, A hydrogen-atom abstraction model for the function of Y_Z in photosynthetic oxygen evolution, *Photosynth. Res.* 46 (1995) 177-185.

[10] G. Bernát, F. Morvaridi, Y. Feyziyev, S. Styring, pH dependence of the four individual transitions in the catalytic S-cycle during photosynthetic oxygen evolution, *Biochemistry* 41 (2002) 5830-5843.

[11] H. Suzuki, M. Sugiura, T. Noguchi, Monitoring proton release during photosynthetic water oxidation in photosystem II by means of isotope-edited infrared spectroscopy, *J. Am. Chem. Soc.* 131 (2009) 7849-7857.

[12] L. Gerencsér, H. Dau, Water oxidation by Photosystem II: H₂O–D₂O and the influence of pH support formation of an intermediate by removal of proton before dioxygen creation, *Biochemistry* 49 (2010) 10098-10106.

[13] I. Zaharieva, J.M. Wichmann, H. Dau, Thermodynamic limitations of photosynthetic water oxidation at high proton concentrations, *J. Biol. Chem.* 286 (2011) 18222-18228.

[14] L. Thompson, G. Brudvig, Cytochrome *b*-559 may function to protect photosystem II from photoinhibition, *Biochemistry* 27(1988) 6653-6658.

[15] C.A. Buser, L.K. Thompson, B.A. Diner, G.W. Brudvig, Electron-transfer reactions in

manganese-depleted photosystem II. *Biochemistry* 29 (1990) 8977-8985.

[16] J. Barber, J. De Las Rivas, A functional model for the role of cytochrome b_{559} in the protection against donor and acceptor side photoinhibition, *Proc. Natl. Acad. Sci. U.S.A.* 90 (1993) 10946-10946.

[17] A. Magnuson, M. Rova, F. Mamedov, P.O. Fredriksson, S. Styring, role of cytochrome b_{559} and tyrosine_D in protection against photoinhibition during in vivo photoactivation of Photosystem II, *Biochim. Biophys. Acta* 1411 (1999) 180-191.

[18] C.A. Tracewell, A. Cua, D.H. Stewart, D.F. Bocian, G.W. Brudvig, Characterization of carotenoid and chlorophyll photooxidation in Photosystem II, *Biochemistry* 40 (2001) 193-203.

[19] P. Faller, C. Fufezan, A.W. Rutherford, Side-path electron donors: Cytochrome b_{559} , chlorophyll Z and β -carotene. *In: Photosystem II: The light-driven water:plastoquinone oxidoreductase*, 2005, pp. 347-364, Springer, Dordrecht, the Netherlands

[20] J. Hanley, Y. Deligiannakis, A. Pascal, P. Faller, A.W. Rutherford, Carotenoid oxidation in photosystem II, *Biochemistry* 38 (1999) 8189-8195.

[21] P. Faller, A. Pascal, A.W. Rutherford, β -carotene redox reactions in Photosystem II: Electron transfer pathway, *Biochemistry* 40 (2001) 6431-6440.

[22] K.E. Shinopoulos, G.W. Brudvig, Cytochrome b_{559} and cyclic electron transfer within photosystem II. *Biochim. Biophys. Acta* 1817 (2012) 66-75.

[23] S. Styring, A.W. Rutherford, In the oxygen-evolving complex of photosystem II the S_0 state is oxidized to the S_1 state by Y_D^+ (Signal II_{slow}). *Biochemistry* 26 (1987) 2401-2405.

[24] I. Vass I, S. Styring, pH dependent charge equilibria between tyrosine-D and the S-states in photosystem II. Estimation of relative midpoint redox potentials. *Biochemistry* 30 (1991) 830-839.

[25] C.A. Buser, B.A. Diner, G.W. Brudvig, Photooxidation of cytochrome b_{559} in oxygen-

evolving photosystem II. *Biochemistry* (1992) 11449-11459.

[26] A.W. Rutherford, A. Boussac, P. Faller, The stable tyrosyl radical in photosystem II: why D? *Biochim. Biophys. Acta* 1655 (2004) 222-230.

[27] I. Vass, Z. Deák, É. Hideg, Charge equilibrium between the water-oxidizing complex and the electron donor tyrosine-D in Photosystem II, *Biochim. Biophys. Acta* 1017 (1990) 63-69.

[28] F. Morvaridi, Y. Feyziyev, G. Bernát, P. Geijer, F. Mamedov, S. Styring, pH-dependent oxidation of Cytochrome *b*₅₅₉ is different in the different S-states, in: *Proceedings of the 12th International Congress on Photosynthesis, 2001, S13-10*, pp. 1-4, CSIRO Publishing, Melbourne, Australia

[29] Y. Feyziyev, B.J. van Rotterdam, G. Bernát, S. Styring, Electron transfer from cytochrome *b*₅₅₉ and tyrosine_D to the S₂ and S₃ states of the water oxidizing complex in photosystem II. *Chemical Physics* 294 (2003) 415-431.

[30] S. Styring, I. Virgin, A. Ehrenberg, B. Andersson, Strong light photoinhibition of electrontransport in Photosystem II. Impairment of the function of the first quinone acceptor, Q_A. *Biochim. Biophys. Acta* 1015 (1990) 269-278.

[31] D.A. Berthold, G.T. Babcock, C.F. Yocum, A highly resolved, oxygen-evolving photosystem II preparation from spinach thylakoid membranes. *FEBS Lett.* 134 (1981) 231-234.

[32] M. Völker, T. Ono, Y. Inoue, G. Renger, Effect of trypsin on the PSII particles. Correlation between Hill activity, Mn-abundance and peptide pattern. *Biochim. Biophys. Acta* 806 (1985) 25-34.

[33] L.K. Thompson, A.F. Miller, C.A. Buser, J.C. de Paula, G.W. Brudvig, Characterization of the multiple forms of cytochrome *b*₅₅₉ in photosystem II. *Biochemistry* 28 (1989) 8048-8056.

- [34] D.H. Stewart, G.W. Brudvig, Cytochrome b_{559} of photosystem II. *Biochim. Biophys. Acta* 1367 (1998) 63-87.
- [35] S. Demeter, J.H.A. Nugent, L. Kovács, G. Bernát, M.C.W. Evans, Comparative EPR and thermoluminescence study of anoxic photoinhibition in Photosystem II particles. *Photosynth. Res.* 46 (1995) 213-218.
- [36] I. Vass, Z. Deák, C. Jegerschöld, S. Styring. The accessory electron donor tyrosine-D of photosystem II is slowly reduced in the dark during low-temperature storage of isolated thylakoids. *Biochim. Biophys. Acta* 1018 (1990) 41-46.
- [37] R. Gadjieva, F. Mamedov, G. Renger, S. Styring, Interconversion of low- and high-potential forms of cytochrome b_{559} in Tris-washed photosystem II membranes under aerobic and anaerobic conditions. *Biochemistry* 38 (1999) 10578-10584.
- [38] G.T. Babcock, K. Sauer, Electron paramagnetic resonance signal II in spinach chloroplasts. I. Kinetic analysis for untreated chloroplasts. *Biochim. Biophys. Acta* 325 (1973) 483-503.
- [39] Z. Deák, I. Vass, S. Styring, Redox interaction of Tyrosine-D with the S-states of the water-oxidizing complex in intact and chloride-depleted Photosystem II. *Biochim. Biophys. Acta* 1185 (1994) 65-74.
- [40] S. Styring, A.W. Rutherford, Deactivation kinetics and temperature dependence of the S-state transitions in the oxygen-evolving system of Photosystem II measured by EPR spectroscopy. *Biochim. Biophys. Acta* 933 (1988) 378-387.
- [41] R.J. Debus, The manganese and calcium ions of photosynthetic oxygen evolution. *Biochim. Biophys. Acta* 1102 (1992) 269-352.
- [42] J.P. McEvoy, G.W. Brudvig, Water-splitting chemistry of photosystem II. *Chem. Rev.* 106 (2006) 4455-4483.

- [43] J. Messinger, G. Renger, Photosynthetic water splitting, in: G. Renger (Ed.) Primary processes of photosynthesis, Part 2, 2008, pp 291-349, RSC Publishing, Cambridge, U.K.
- [44] H. Dau, M. Haumann, The manganese complex of photosystem II in its reaction cycle – Basic framework and possible realization at the atomic level. *Coord. Chem. Rev.* 252 (2008) 273-295.
- [45] G. Renger, T. Renger, Photosystem II: The machinery of photosynthetic water splitting. *Photosynth. Res.* 98 (2008) 53-80.
- [46] G. Renger, Light induced oxidative water splitting in photosynthesis: Energy, kinetics and mechanism. *J. Photochem. Photobiol. B* 104 (2011) 35-43.
- [47] M. Haumann, C. Müller, P. Liebisch, L. Iuzzolino, J. Dittmer, M. Grabolle, T. Neisius, W. Meyer-Klaucke, H. Dau, Structural and oxidation state changes of the photosystem II manganese complex in four transitions of the water oxidation cycle ($S_0 \rightarrow S_1$, $S_1 \rightarrow S_2$, $S_2 \rightarrow S_3$, $S_{3,4} \rightarrow S_0$) characterized by X-ray absorption spectroscopy at 20 K and room temperature. *Biochemistry* 44 (2005) 1894-1908.
- [48] M.H. Vos, Ph.D. Thesis, 1990, University of Leiden, Leiden, the Netherlands
- [49] P. Geijer, F. Morvaridi, S. Styring, The S_3 state of the oxygen-evolving complex in photosystem II is converted to the $S_2Y_Z^\bullet$ state at alkaline pH. *Biochemistry* 40 (2001) 10881-10891.
- [50] T.J. Meyer, M.H.V Huynh, H.H. Thorp, The possible role of proton-coupled electron transfer (PCET) in water oxidation by photosystem II. *Angew. Chem. Int. Ed.* (2007) 5284-5304.

Figure legends

Fig. 1. Schematic view of the electron transport pathway through PSII. For details see text.

Fig. 2. EPR spectra of Y_D^\bullet (A) and ML-S₂ (B) recorded in chemically reduced PSII membranes. Spectra *a*, non-illuminated sample; spectra *b* and *c*, samples excited by 1 and 2 flashes, respectively. Spectrum “*max*” represent the maximal signal intensity of Y_D^\bullet radical obtained by 1 min illumination (room light) and 5 min subsequent dark incubation at room temperature of a chemically reduced sample. The arrow(s) indicate the hyperfine peak(s) which was/were used to determine the amplitude of Y_D^\bullet and the ML-S₂ signal, respectively. EPR settings: Y_D^\bullet , microwave power, 1 μ W; microwave frequency, 9.47 GHz; field modulation amplitude, 3.2 G; temperature, 15 K; ML-S₂, microwave power, 13.1 mW; microwave frequency, 9.47 GHz; field modulation amplitude, 20 G; temperature, 7 K.

Fig. 3. EPR spectra of oxidized Cyt *b*₅₅₉ in 1-flash (A) and 2-flash (B) samples recorded immediately after the flashes (spectra *a*), and after 40 and 163 days of dark incubation at 195 K (spectra *b* and *c*, respectively). The bars indicate the field position of HP (left bar; *g* = 3.05; 2205 G) and LP (right bar; *g* = 2.97; 2255 G) Cyt *b*₅₅₉, respectively. EPR settings: microwave power, 5.3 mW; microwave frequency 9.47 GHz, field modulation amplitude 16 G, temperature 15 K.

Fig. 4. (A) Effect of prolonged dark incubation at 195 K on the signal intensity of the ML-S₂ (circles), Cyt *b*₅₅₉ (triangles) and Y_D^\bullet radical (squares) in a 1-flash sample (initially enriched in the $Y_D^{\text{red}}S_2$ state). The experimental points were fitted either with a single exponential decay (S₂) or rise to a maximum (Cyt *b*₅₅₉ and Y_D^\bullet) (for details see [29] and text). (B) Comparative analysis of the ML-S₂ decay and Cyt *b*₅₅₉ oxidation. The points are fitted with a two-segment linear function.

Fig. 5. (A) Effect of prolonged dark incubation at 195 K on the signal intensity of the ML-S₂ (circles), Cyt *b*₅₅₉ (triangles) and Y_D[•] radical (squares) in a 2-flash sample (initially enriched in the Y_D^{red}S₃ state). Changes in the ML-S₂ intensity during the first 40 days of dark incubation are shown as an inset. The time-course of the increase of the Cyt *b*₅₅₉ and Y_D[•] signals was fitted with an exponential rise to a maximum, while the ML-S₂ intensities in the inset are fitted by a biphasic decay (for details see [29]). (B) Comparative analysis of the S₃ decay and Cyt *b*₅₅₉ oxidation. The S₃ population size at certain time points (inset) is estimated by using the determined initial S₃ population size (~55%) and the rate constant of the S₃→S₂ decay ($k_1 \approx 0.055 \text{ d}^{-1}$). The experimental points on the main panel are fitted with a hyperbolic function. (C) Comparative analysis of the S₁ formation during the decay of higher S-states and Cyt *b*₅₅₉ oxidation. The S₁ population is estimated by taking into account the measured S₂ (panel A) and predicted S₃ (inset on panel B) populations. The points are fitted with a two-segment linear function.

Fig. 6. Decays of the higher S-states at 195 K. Oxidation of the major and minor redox partners are indicated by solid and dotted semicircular arrows, respectively. For further details, see text.

Figures

Figure 1

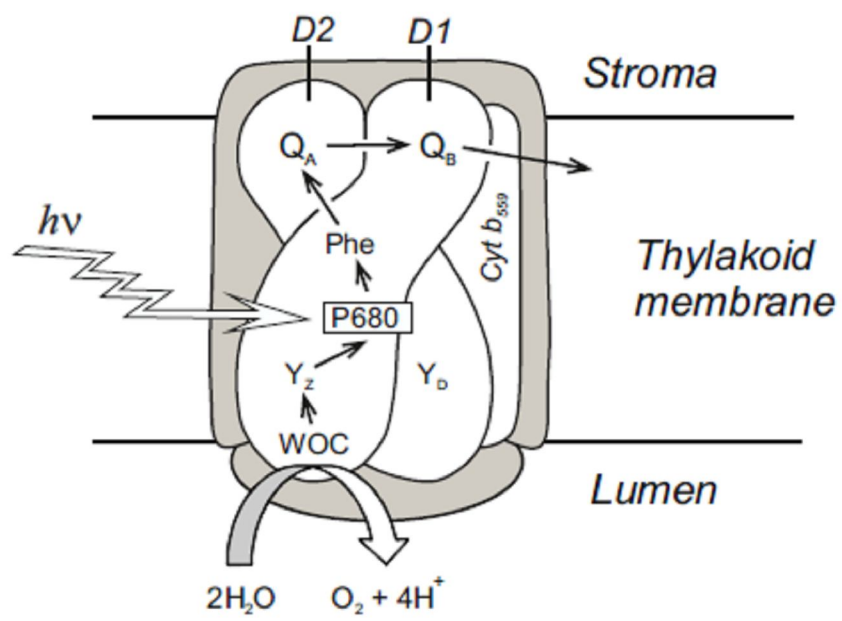


Figure 2A

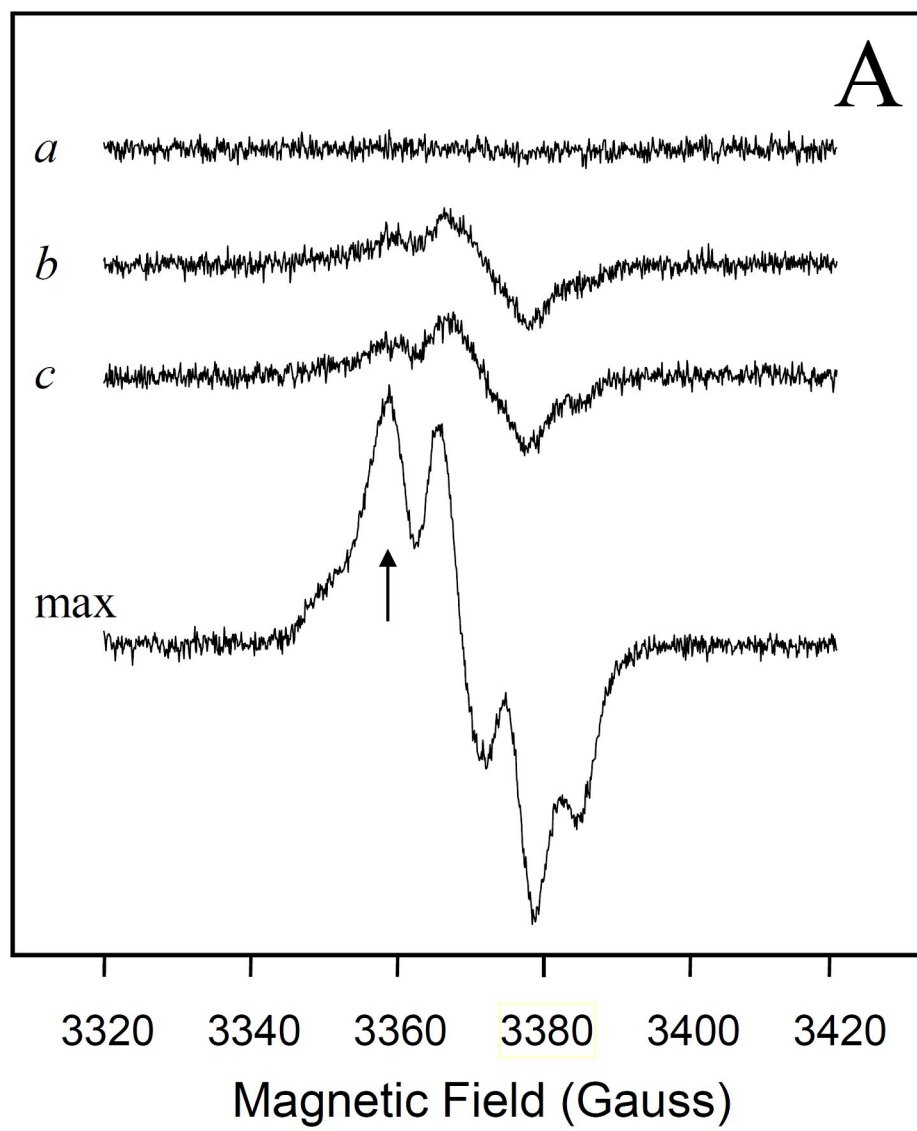


Figure 2B

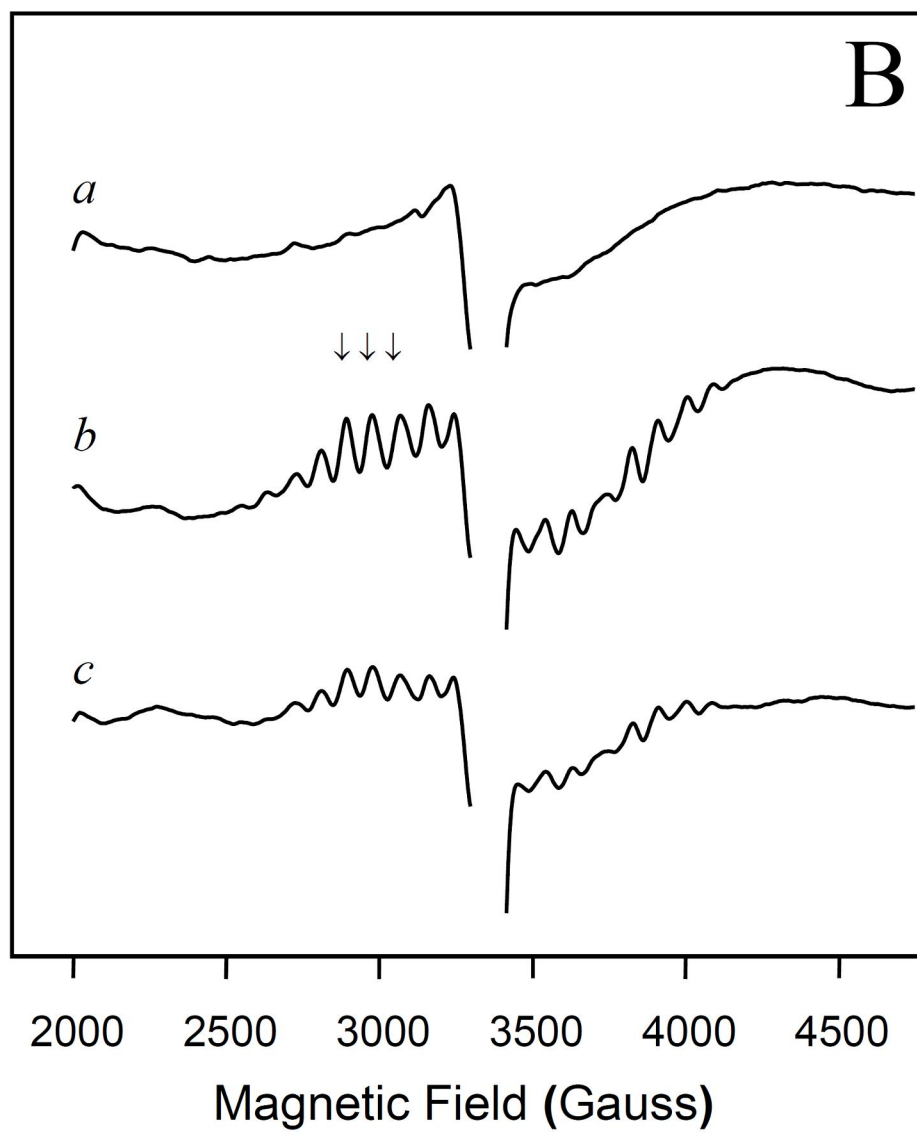


Figure 3A

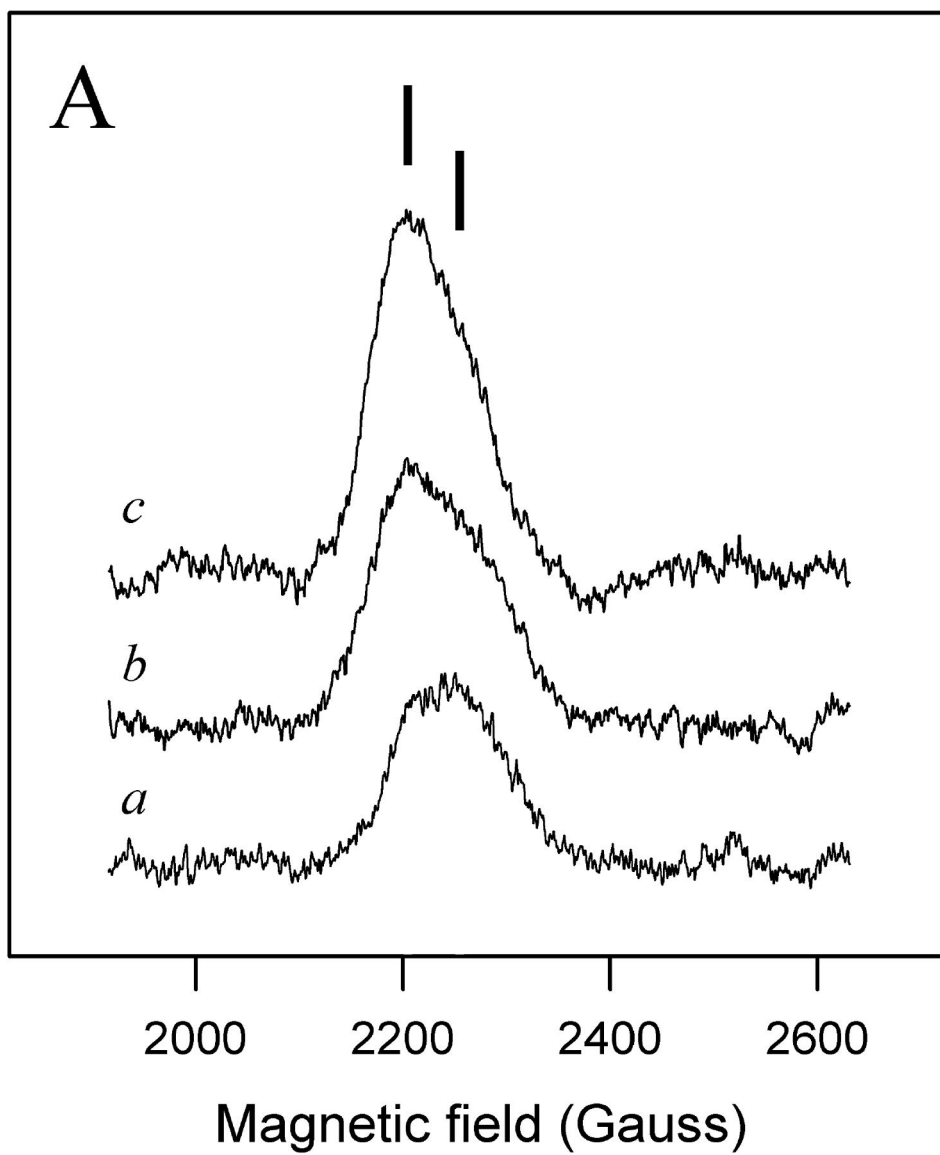


Figure 3B

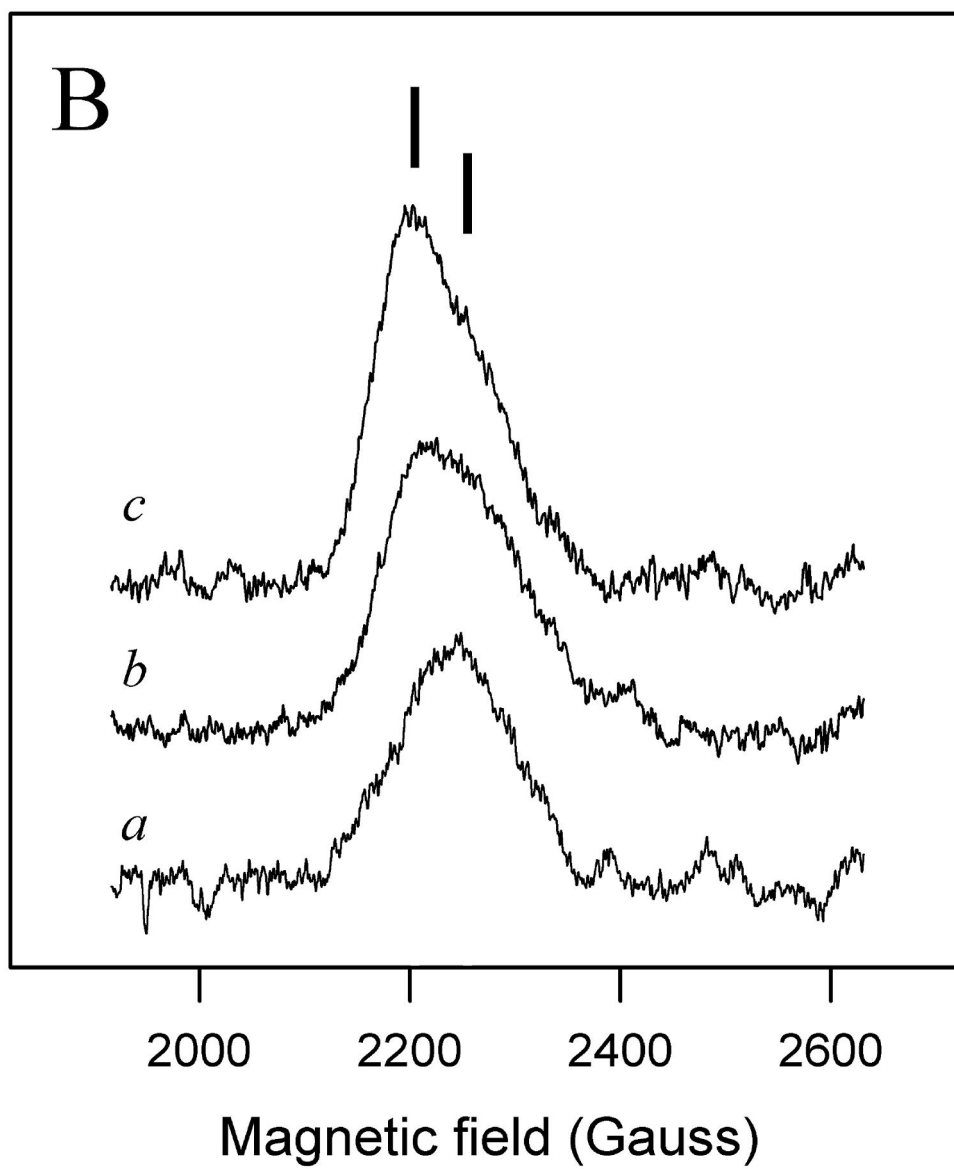


Figure 4A

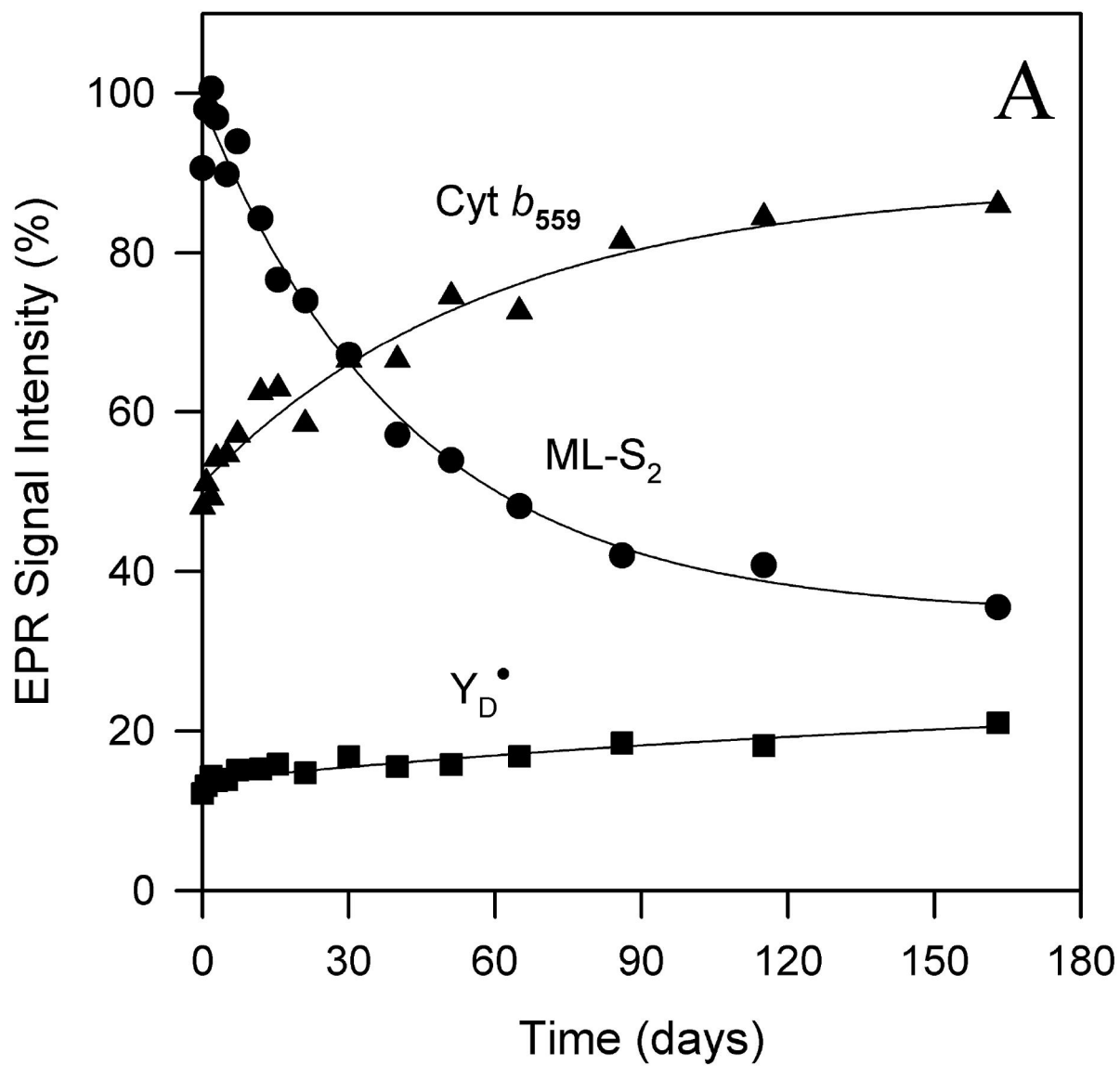


Figure 4B

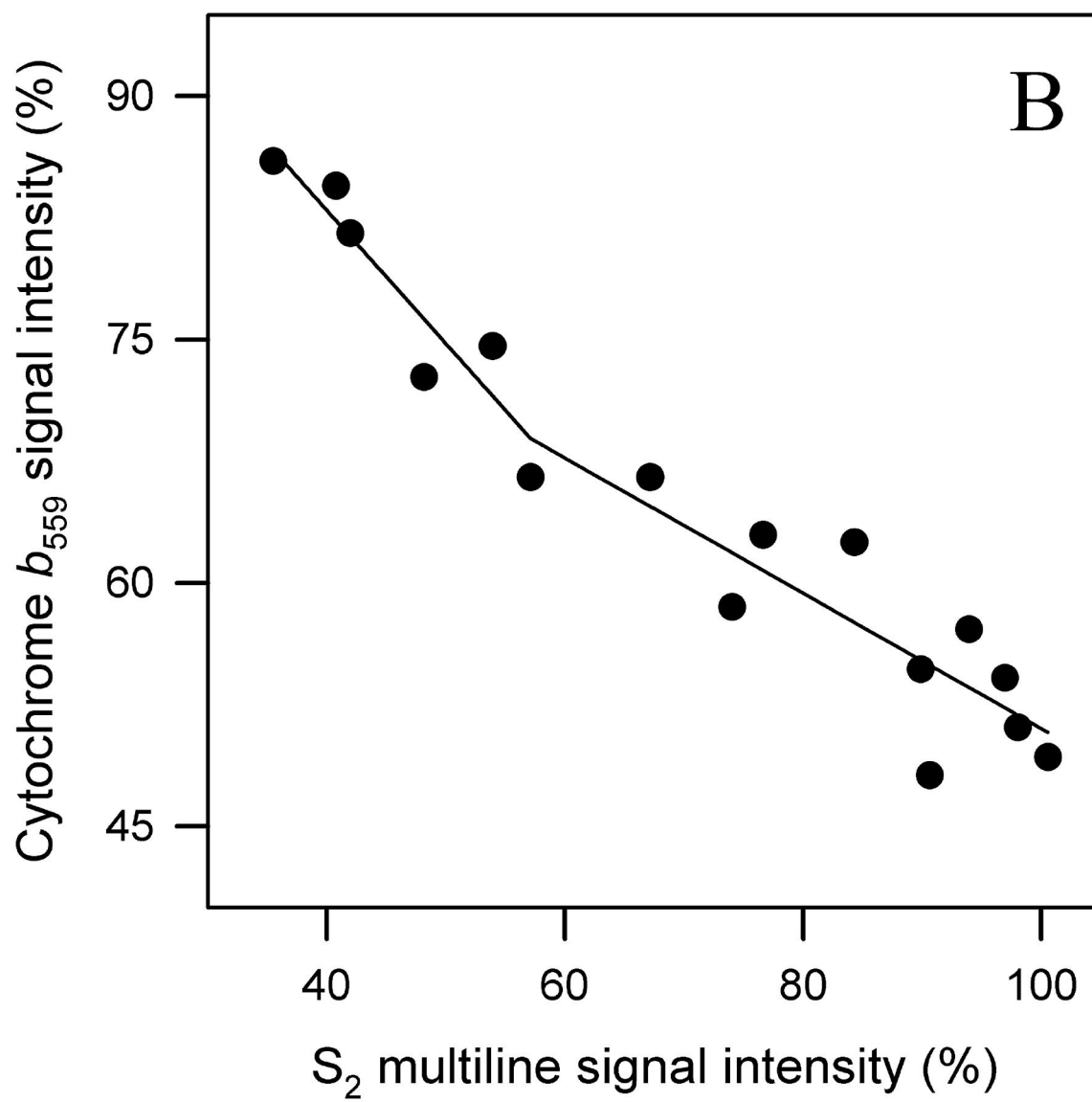


Figure 5A

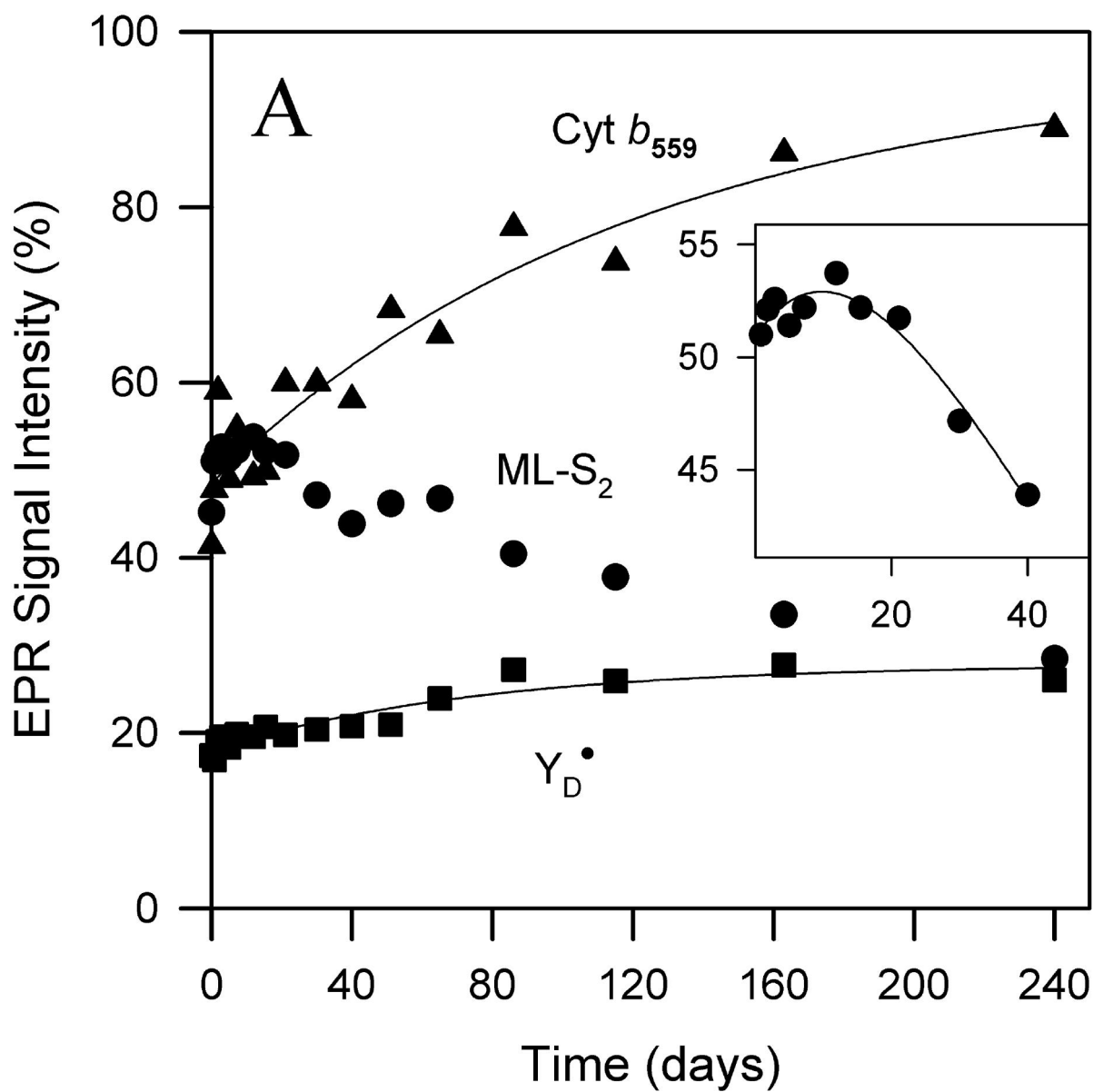


Figure 5B

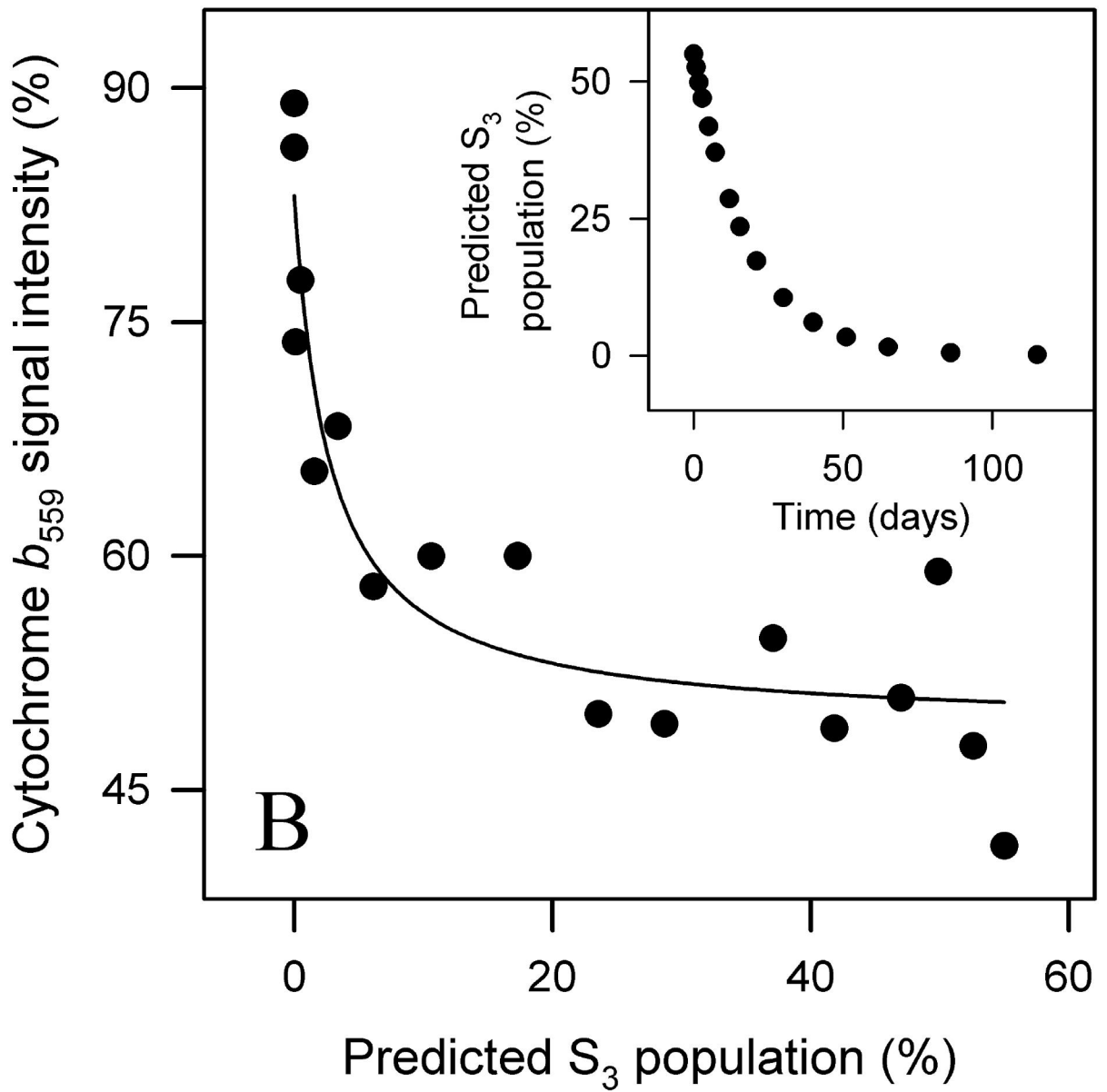


Figure 5C

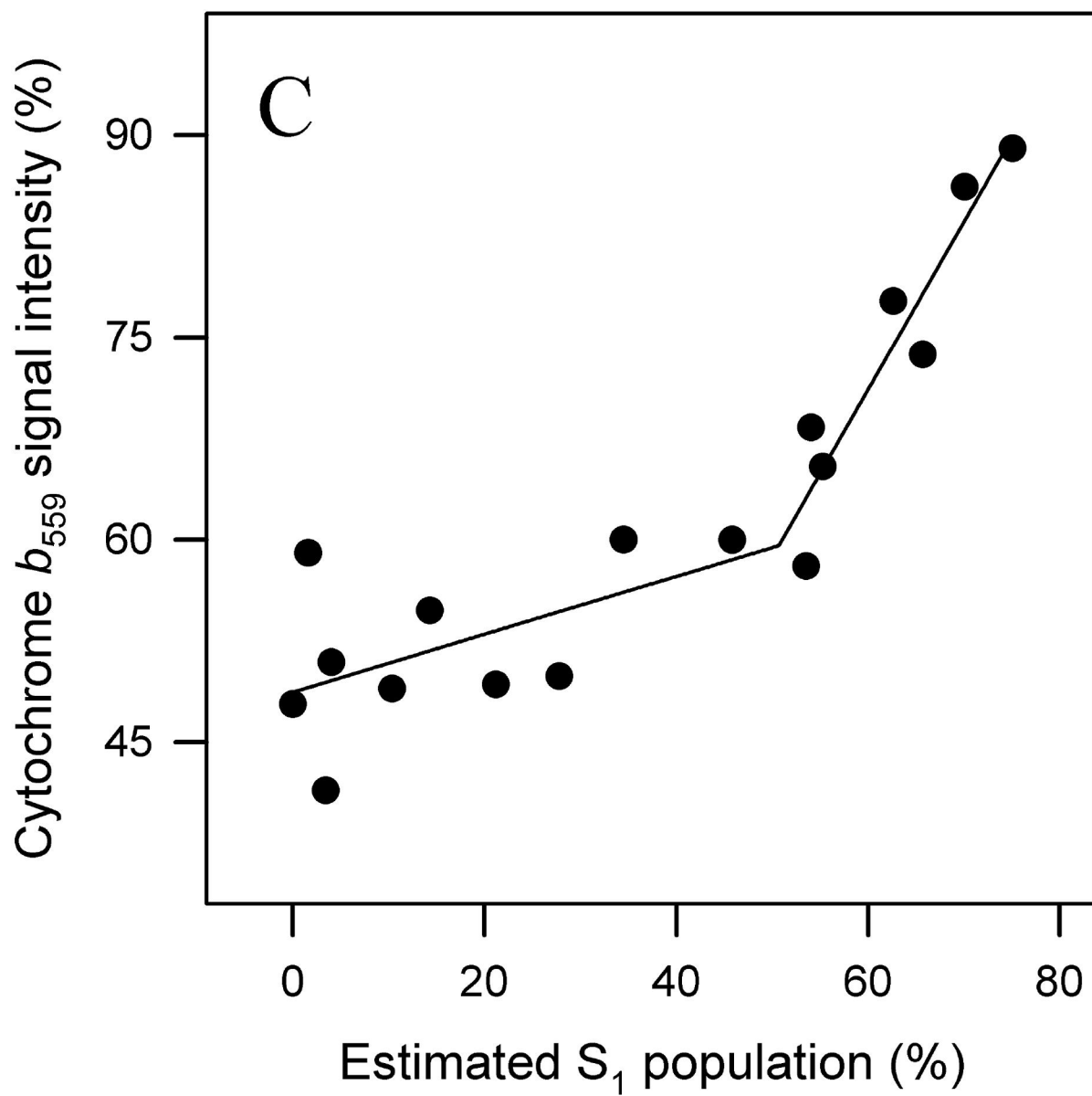


Figure 6

